AARSs are a ubiquitously expressed, essential family of enzymes responsible for attaching amino acids to their cognate tRNAs in all cells and tissues. Mutations in 4 genes, *GARS*, *YARS*, *AARS*, and *KARS*, that encode AARSs have been implicated in CMT/dHMN.[5,8–10] Mutations in *GARS*, *YARS*, and *AARS* cause autosomal dominant CMT/dHMN. Two *KARS* mutations were detected in the compound heterozygous state in a patient with autosomal recessive CMT, developmental delay, self-abusive behavior, dysmorphic features, and vestibular schwannoma.[10] To elucidate the reason that mutations in ubiquitously expressed AARSs result in peripheral neuropathy, the effects of GARS, YARS, AARS, and KARS mutations in CMT/dHMN were investigated. A common pathologic mechanism for genetic disorders is a loss of gene function through altered mRNA or protein levels, although this is unusual for neurodegenerative diseases inherited in an autosomal dominant manner. Studies on G240R GARS heterozygous mutated lymphoblastoid cells did not reveal severely altered transcription, translation, or protein stability.[12] Pathogenic mechanisms such as defective aminoacylation, abnormal distribution in axons, or a combination of both are postulated to underlie CMT/dHMN, based on functional and protein localization studies of heterozygous GARS and AARS mutants.[9,12] Functional analyses of compound heterozygous mutations in *KARS* revealed severely affected enzyme activity.[10]

AARS catalyzes the attachment of alanine to its cognate tRNAs during protein synthesis. Investigation of the structure of AARS by X-ray crystallography revealed that it contains, from the N to the C terminus, an aminoacylation domain, a middle helical domain, an editing domain, and a so-called C-Ala domain.[13] The reported variant (R329H) is located in the middle helical domain, which together with the aminoacylation domain, is responsible for the complete and specific aminoacylation of AARS. The D893N variation is located in the C-Ala domain, which facilitates efficient editing by bringing together the aminoacylation and editing domains. A sequence homology search was performed to align protein sequences from multiple species, using a constraint-based multiple alignment tool (COBALT) (http://www.ncbi.nlm.nih.gov/tools/cobalt/). Aspartic acid 893 was conserved among all species analyzed (figure 2H). Thus, the D893N mutation identified in the Chinese dominant dHMN family is located in a remarkably well-conserved sequence of amino acids, suggesting that it may have a potential functional impact on AARS. Furthermore, we were able to computationally predict the effect of the D893N mutation on protein function using the MuPro (http://www.ics.uci.edu/~baldig/mutation.html) and PolyPhen-2 (http://genetics.bwh.harvard.edu/pph2/) algorithms, which gave scores of −0.334 and 0.802, respectively. MUPro scores of less than 0 indicate a decrease in protein stability, and PolyPhen-2 scores of approximately 1 indicate a prediction of pathogenicity. The D893N mutation is probably a pathogenic mutation, based on the degree of conservation of the affected residues.

Five genes (*HSPB8, HSPB1, GARS, TRPV4*, and *BCSL2*) have been described in both dHMN and CMT.[2–7] We add *AARS* on the basis of the present report. GARS and AARS are involved in common processes during protein synthesis, and the mutations reported to date were all missense mutations. Pathogenic missense mutations for autosomal dominant disease usually have a gain-of-function or dominant-negative effect. These pathogenic mutations of tRNA synthetases may directly disrupt protein synthesis.

Our data confirm that a mutation in the *AARS* gene (designated p.D893N) is associated with dominant dHMN in a Chinese family. This observation adds to a growing body of evidence that implicates specific genes/proteins in peripheral nerve function and delineates the pathologic consequences of their dysfunction.

AUTHOR CONTRIBUTIONS

Z. Zhao and Dr. Hashiguchi contributed equally to this work. Dr. Hu and Dr. Takashima designed the research. Z. Zhao, Dr. Hashiguchi, Dr. Tokunaga, Dr. Sakiyama, and Dr. Okamoto performed genetic studies. L. Zhu, H. Shen, and Dr. Hu performed clinical research and provided patient information. Z. Zhao, Dr. Hu, and Dr. Takashima wrote the article.

ACKNOWLEDGMENT

The authors thank the families described in this report for their cooperation and A. Yoshimura of Kagoshima University for her excellent technical assistance.

DISCLOSURE

The authors report no disclosures relevant to the manuscript. **Go to Neurology.org for full disclosures.**

Received October 18, 2011. Accepted in final form January 23, 2012.

REFERENCES

1. Harding AE. Inherited neuronal atrophy and degeneration predominantly of lower motor neurons. In: PJ Dyck, PK Thomas, eds. Peripheral Neuropathy. Philadelphia: WB Saunders; 1993.
2. Drew AP, Blair IP, Nicholson GA. Molecular genetics and mechanisms of disease in distal hereditary motor neuropathies: insights directing future genetic studies. Curr Mol Med 2011;11:650–665.
3. Irobi J, Van Impe K, Seeman P, et al. Hot-spot residue in small heat-shock protein 22 causes distal motor neuropathy. Nat Genet 2004;36:597–601.
4. Houlden H, Laura M, Wavrant-De Vrièze F, et al. Mutations in the HSP27 (HSPB1) gene cause dominant, reces-

sive, and sporadic distal HMN/CMT type 2. Neurology 2008;71:1660–1668.
5. Antonellis A, Ellsworth RE, Sambuughin N, et al. Glycyl tRNA synthetase mutations in Charcot-Marie-Tooth disease type 2D and distal spinal muscular atrophy type V. Am J Hum Genet 2003;72:1293–1299.
6. Windpassinger C, Auer-Grumbach M, Irobi J, et al. Heterozygous missense mutations in BSCL2 are associated with distal hereditary motor neuropathy and Silver syndrome. Nat Genet 2004;36:271–276.
7. Sambuughin N, Sivakumar K, Selenge B, et al. Autosomal dominant distal spinal muscular atrophy type V (dSMA-V) and Charcot-Marie-Tooth disease type 2D (CMT2D) segregate within a single large kindred and map to a refined region on chromosome 7p15. J Neurol Sci 1998;161:23–28.
8. Jordanova A, Irobi J, Thomas FP, et al. Disrupted function and axonal distribution of mutant tyrosyl-tRNA synthetase in dominant intermediate Charcot-Marie-Tooth neuropathy. Nat Genet 2006;38:197–202.
9. Latour P, Thauvin-Robinet C, Baudelet-Méry C, et al. A major determinant for binding and aminoacylation of $tRNA^{Ala}$ in cytoplasmic alanyl-tRNA synthetase is mutated in dominant axonal Charcot- Marie-Tooth disease. Am J Hum Genet 2010;86: 77–82.
10. McLaughlin HM, Sakaguchi R, Liu C, et al. Compound heterozygosity for loss-of-function lysyl-tRNA synthetase mutations in a patient with peripheral neuropathy. Am J Hum Genet 2010;87:560–566.
11. Cutler DJ, Zwick ME, Carrasquillo MM, et al. High-throughput variation detection and genotyping using microarrays. Genome Res 2001;11:1913–1925.
12. Antonellis A, Lee-Lin SQ, Wasterlain A, et al. Functional analyses of glycyl-tRNA synthetase mutations suggest a key role for tRNA-charging enzymes in peripheral axons. J Neurosci 2006;26:10397–10406.
13. Swairjo MA, Otero FJ, Yang XL, et al. Alanyl-tRNA synthetase crystal structure and design for acceptor-stem recognition. Mol Cell 2004;13:829–841.

1）Charcot-Marie-Tooth 病の網羅的遺伝子診断

鹿児島大学大学院医歯学総合研究科神経内科・老年病学講座　橋口昭大
同　教授　高嶋　博

key words　microarray DNA chip, next generation genome sequencer, *PMP22* duplication, *MFN2*, aminoacyl-tRNA synthetase

要　旨

Charcot-Marie-Tooth病（CMT）の原因遺伝子は30以上報告されており，臨床的および遺伝子学的に多様である．CMTの最も多い原因である*peripheral myelin protein 22* (*PMP22*) の異常は外注委託検査によるfluorescence *in situ* hybridization（FISH）法で検出可能であるが，その他の遺伝子異常を全てスクリーニングするには膨大な労力と費用が必要である．本邦では，従来通常のシークエンス法やDHPLC（denaturing high performance liquid chromatography）法による遺伝子診断が行われてきたが，これらに加えてCMTの遺伝子異常を低コストかつ迅速に診断できるマイクロアレイDNAチップが開発され，27の遺伝子を同時にスクリーニング可能となった．その結果おおよその原因遺伝子頻度が発表されるにいたった．一方，米国においても詳細なCMTの遺伝子診断が行われ，病型別のおおよその原因遺伝子頻度が発表された．これらから，総合的な遺伝子異常の検出割合は，*PMP22*の重複例であるCMT1Aを除けば約20%であり，原因遺伝子が未解明の症例が多いことが確認された．それ故，今後も新しい原因遺伝子の同定が必要と考えられ，実際に毎年複数の新規原因遺伝子が報告されている．2010年には次世代シークエンサーを用い，個人のゲノム全塩基配列を解読することで，SH3TC2遺伝子変異によるCMT4Cと確認しえた初めての報告がなされた[1]．今後，次世代シークエンサーなどの網羅的遺伝子診断により，原因遺伝子の発見が加速し，包括的な遺伝子診断にも利用されていくことが期待される．

動　向

1991年にLupskiらが*PMP22*の重複がCMT1Aの原因であると報告[2]して以来，すでに30以上のCMT原因遺伝子が報告されている（表1）．欧米では，いくつかのCMT原因遺伝子診断を，従来のSanger法のシークエンス解析を用いて商業的に行っている．一方，本邦ではPMP22以外の遺伝子診断は商業的には行われていないが，近年，CMT原因遺伝子を網羅的にスクリーニングする試みが行われている．マイクロアレイDNAチップを用いた手法では，DNAチップ上に搭載された27のCMT原因遺伝子を最短2日で診断可能で，注目されている．

一方，本邦とアメリカでの遺伝子解析にて，原因遺伝子の多様性および病型別遺伝子頻度が報告されており，本稿で概説する．また，近年相次い

表1　Charcot-Marie-Tooth病の原因遺伝子（文献19より改変）

CMT 1（脱髄型 常優）	
CMT1A	*PMP22 (peripheral myelin protein 22)*
CMT1B	*MPZ (myelin protein zero)*
CMT1C	*LITAF (lipopolysaccharide-induced TNF factor)*
CMT1D	*EGR2 (early growth response 2)*
CHN	*SOX10 (sex determining region Y-box 10)*
CMT1E	*MPZ (myelin protein zero)*
CMT1F	*NEFL (neurofilament, light polypeptide)*
CMT 4（脱髄型 常劣）	
CMT4A	*GDAP1 (ganglioside-induced differentiation associated protein 1)*
CMT4B1	*MTMR2 (myotubularin related protein 2)*
CMT4B2	*SBF2 (SET binding factor 2)*
CMT4C	*SH3TC2 (SH3 domain and tetratricopeptide repeats 2)*
CMT4D	*NDRG1 (N-myc downstream regulated 1)*
CMT4E	*EGR2 (early growth response 2)*
CMT4F	*PRX (periaxin)*
CMT4G	*HK1 (hexokinase 1)*
CMT4H	*FGD4 (FYVE, RhoGEF and PH domain containing 4)*
CMT4J	*FIG4 (FIG4 homolog, SAC1 lipid phosphatase domain containing)*
CMT X（X連鎖性）	
CMTX1	*GJB1 (gap junction binding protein beta 1)*
CMTX5	*PRPS1 (phosphoribosyl pyrophosphate synthetase 1)*
CMT 2（軸索型 常優）	
CMT2A1	*KIF1B (kinesin family member 1B)*
CMT2A2	*MFN2 (mitofusin 2)*
CMT2B	*RAB7 (rab-protein 7)*
CMT2C	*TRPV4 (transient receptor potential cation channel, subfamily V, member 4)*
CMT2D	*GARS (glycyl-tRNA synthetase)*
CMT2E	*NEFL (neurofilament, light polypeptide)*
CMT2F	*HSPB1 (heat shock 27kDa protein 1)*
CMT2G	*unknown*
CMT2H	*unknown*
CMT2I/J	*MPZ (myelin protein zero)*
CMT2K	*GDAP1 (ganglioside-induced differentiation associated protein 1)*
CMT2L	*HSBP8 (heat shock 22kDa protein 8)*
CMT2M	*DNM2 (dynamin 2)*
CMT2N	*AARS (alanyl-tRNA synthetase)*
CMT 2（軸索型 常劣）	
AR-CMT2A	*LMNA (lamin A/C)*
AR-CMT2B	*MED25 (mediator complex subunit 25)*
GAN	*GAN1 (gigaxonin 1)*
ACCPN	*KCC3 (K-Cl cotransporter family 3)*
SCAN1	*TDP1 (tyrosyl-DNA phosphodiesterase 1)*
AOA1	*APTX (aprataxin)*
AOA2	*SETX (senataxin)*
minifascicular neuropathy	*DHH (desert hedgehog)*
CMT 2（中間型）	
CMT DIB	*DNM2 (dynamin 2)*
CMT DIC	*YARS (tyrosyl-tRNA synthetase)*

CHN: congenital hypomyelinating neuropathy, GAN: giant axonal neuropathy, ACCPN: agenesis of the corpus callosum with peripheral neuropathy, SCAN: spinocerebellar ataxia with axonal neuropathy, AOA: ataxia with oculomotor apraxia

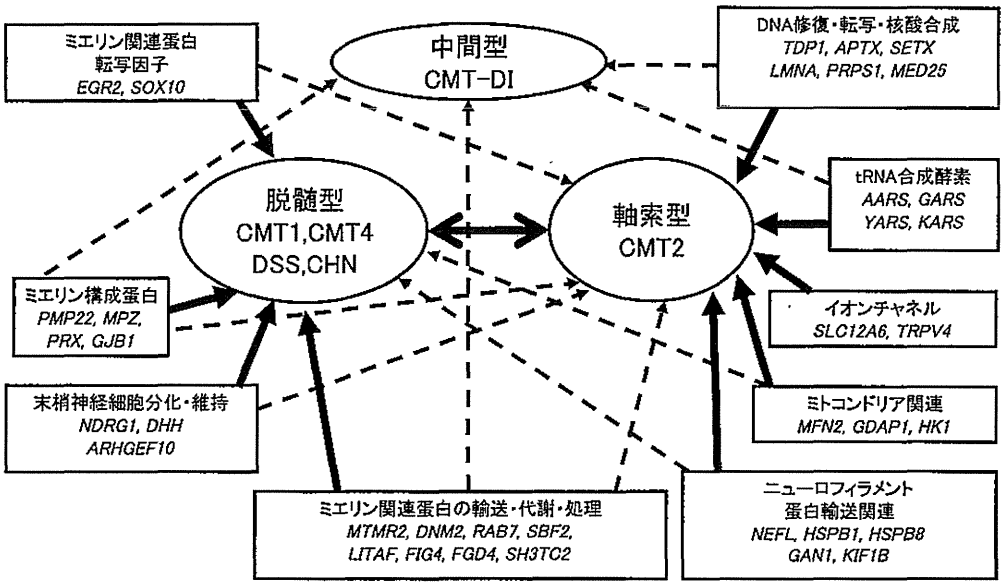

図1　Charcot-Marie-Tooth 病の病態別遺伝子分類（文献19より改変）

で発見された注目すべき原因遺伝子に関する知見と，マイクロアレイDNAチップによる網羅的遺伝子診断法の特性と問題点についても概説する．

A. 原因遺伝子の多様性

CMTの原因遺伝子はすでに30を超えている（表1）．それらの遺伝子は病態別に，①ミエリン構成蛋白，②ミエリン関連蛋白転写因子，③ミエリン関連蛋白の輸送・代謝・処理，④細胞分化・維持，⑤ニューロフィラメント・蛋白輸送関連，⑥ミトコンドリア関連，⑦DNA修復・転写・核酸合成，⑧イオンチャネル，⑨アミノアシルtRNA合成酵素のおおよそ9つに分類できる．①～④はミエリン形成に関する遺伝子で，主に脱髄型CMTの原因に，⑤～⑨は神経細胞の形成・維持・活動に関連する遺伝子で，主に軸索型CMTの原因となる．図1に示すように，これら原因遺伝子によっては脱髄型と軸索型いずれの病型もとりうるため，数多くのCMTサブタイプが報告されている．

B. CMTの分子疫学

CMTは電気生理学的所見，病理学的所見，発症年齢，家族歴，進行経過，合併症などから原因遺伝子をある程度推定できるが，必ずしも想定した遺伝子に異常を認めないことも多い．

Saportaらは，遺伝子診断を行ったCMT患者787例の疫学解析を行い，CMT1が45%（354例），CMT2が12.2%（96例），CMTXが10.2%（80例），CMT4が0.9%（7例）と報告している[3]．CMT1が最多で，そのうち約82%（290/354例）が*PMP22*重複によるCMT1Aであった．CMT1Aについて，Szigetiらは米36施設で遺伝子診断されたCMTにおいて，脱髄型CMTの約70%がCMT1Aであると報告し[4]，Onishiらはアジア/コーカシアンにおいても脱髄型CMTの約70%がCMT1Aであると報告している[5]．これらの報告からは脱髄型CMTにおけるCMT1Aの割合は世界共通に約70～80%であると推定される．また，Boerkoelらは，商業的な遺伝子診断が開始される以前の検体について検討し，CMT患者153例

のうち，約半数（79例）がCMT1Aであったと報告している[6]．一方，近年Abeらは本邦での脱髄型CMT患者227例のうち，CMT1Aは約23%（53例）であったとし，本邦では世界的な比率より低い可能性を示唆した[7]．実際には23%という頻度はこれまでの報告と比べ低すぎるように見受けられる．本邦ではCMT1Aのみ商業的な遺伝子検査が行われている点や小児科領域からの報告であることなどのバイアスが存在する可能性は否定できない．CMT1A以外の脱髄型CMTについて，Saportaらの報告[3]では*MPZ*変異によるCMT1Bが約13%（45/354例）で認められた以外はいずれも0.3～1.4%と稀であった．Abeらの論文[7]においてもCMT1Bが脱髄型CMTの約9%（20/227例）と多かった．筆者らによるCMT1A以外のCMT患者200例のマイクロアレイ法による網羅的遺伝子診断の結果[8]では，CMT1A以外の脱髄型CMTの約12.8%（6/47例）が*MPZ*変異によるCMT1Bであった．CMT1Aを除いた脱髄型CMTにおけるCMT1Bの頻度は3つの報告[3,7,8]で同等であった．

軸索型CMTについて，Saportaらの報告[3]では，約22%（21/96例）が*Mitofusin-2*（*MFN2*）変異によるCMT2Aであった．Abeらの報告[7]でも約11%（14/127例）がCMT2Aであった．筆者らの報告[8]においても軸索型CMTの約11.3%（8/71例）に*MFN2*変異を認め，Abeら[7]とほぼ同様の結果であった．CMT2A以外の軸索型CMTは，3つの報告[3,7,8]において，いずれの遺伝子も5%未満と少なかった．Saportaらの報告[3]は対象数が非常に多い点，Abeらの報告[7]は日本人で評価した点が重要である．

一方，これら論文に共通する点として，原因遺伝子が特定できない症例が依然として多い点があげられる．Boerkoelら[6]は約29%（44/153例）のCMT患者が原因不明だったとしているが，CMT1Aの79例を除くと実に約60%（44/74例）が原因不明である．Abeらの報告[7]でも，原因不明の脱髄型CMTは約49%（111/227例）であるが，CMT1Aを除くと約64%（111/174例）が原因不明である．さらに軸索型CMTの約79%（100/127例）の原因が特定できていない．Saportaらの報告[3]では，原因不明の脱髄型CMTは約2%（8/354例）と低かったが，軸索型CMTは約66%（63/96例）が原因不明であった．筆者らの報告[8]でも，CMT1Aを除いた脱髄型CMTの約81%（38/47例）が原因不明であり，既報告と同様あるいはそれ以上に多かった．軸索型CMTも約86%（61/71例）が原因不明であった．このように，脱髄型，軸索型CMTともにその多くはいまだ原因遺伝子が同定できていないのが現状である．

C. 新規原因遺伝子

以下に2007年以降に報告された，新規の原因遺伝子をあげる．

FIG4 homolog, SAC1 lipid phosphatase domain containing (*FIG4*), *FYVE, RhoGEF and PH domain containing 4* (*FGD4*) はミエリン関連蛋白の輸送・代謝・処理に関する蛋白である．FIG4はホスファチジルイノシトール代謝に関連し，CMT4J[9]の原因遺伝子である．FGD4はシュワン細胞の分化調節に関連し，CMT4H[10]の原因遺伝子である．

Hexokinase 1 (*HK1*) はミトコンドリア関連遺伝子で，ミトコンドリアの移動やグルコース代謝に関連し，CMT4G / HMSN-Russe[11]の原因遺伝子である．

Phosphoribosyl pyrophosphate synthetase 1 (*PRPS1*) は，X染色体上にあるDNA修復・転写および核酸合成関連遺伝子で，プリン・核酸代謝に関連し，CMTX5[12]の原因遺伝子である．*Mediator complex subunit 25* (*MED25*) もDNA

修復・転写および核酸合成関連遺伝子で，RNAポリメラーゼIIを介する転写に関連する．AR-CMT2B[13]の原因遺伝子である．

Transient receptor potential cation channel, subfamily V, member 4 (*TRPV4*) はイオンチャネル関連遺伝子で，Ca^{2+}浸透圧性カチオンチャネルをコードし，浸透圧調整に関与する．2010年にCMT2C[14]の原因遺伝子として同定された．

Alanyl-tRNA synthetase (*AARS*) と*Lysyl-tRNA synthetase* (*KARS*) はアミノアシルtRNA合成酵素をコードする遺伝子で，AARSはCMT2N[15]の，また*KARS*はCMT-RIB[16]の原因遺伝子として2010年に同定された．アミノアシルtRNA合成酵素は特定のアミノ酸とtRNAを結合させ，アミノアシル化させるために必要な酵素である．*AARS*, *KARS*の同定以前に，*Glycyl-tRNA synthetase* (*GARS*) はCMT2D[17]の原因遺伝子として，*Tyrosyl-tRNA synthetase* (*YARS*) はCMT-DIC[18]の原因遺伝子としてすでに同定されていた．これら以外にも各アミノ酸に対応するアミノアシルtRNA合成酵素は存在しており，今後，新たなCMT原因遺伝子として同定される可能性が高い．アミノアシルtRNA合成酵素異常による慢性的な蛋白供給不足が，転写要求が高い大型の神経細胞を傷害し，軸索型CMTを発症する機序は大変興味深い．

D. 網羅的遺伝子診断法

本邦では，FISH法による*PMP22*遺伝子診断が保険適応となっており，外注委託検査で容易に診断可能である．一方，CMT1A以外のCMTは，各研究施設が個別に遺伝子解析を実施しているのが現状である．電気生理検査所見・末梢神経病理所見・家族歴などの患者情報から原因遺伝子を推測することは，一部の例では可能であるが，同じ原因遺伝子でも脱髄型あるいは軸索型を呈することもあり，また*de novo*変異も少なくない．したがって，患者情報から原因遺伝子を特定するのは困難である．これまでの網羅的遺伝子診断に関する報告で[3-7]は，FISH法の他に，Sanger法シークエンス，denaturing high performance liquid chromatography (DHPLC) 法，multiplex ligation-dependent probe analysis (MLPA) 法などを組み合わせてスクリーニングを行っている一方，個々の症例に対して，これらの方法で30を超す原因遺伝子全てをスクリーニングすることは労力的にもコスト的に困難である．特に一般的なSanger法では莫大な費用と時間を要し，現時点で，全ての原因遺伝子をスクリーニングすることは現実的に不可能である．

DHPLC法は，液体クロマトグラフィーと厳密な温度コントロール可能なオーブンと特殊なDNA分離カラムを組み合わせ，遺伝子異常を同定する方法である．より簡便に実施できるように設計され，高感度，ハイスループット，比較的低ランニングコストという特徴がある．DHPLC法は，シークエンスの必要な検体を簡単に減らせられるという点で，有用なスクリーニング法の一つであろう．

一方，近年のマイクロアレイ法を用いたリシークエンス技術の発展により，高速かつ低コストで網羅的に遺伝子配列を決定することが可能となった．マイクロアレイ法は，目的遺伝子をPCR法で増幅し，それを断片化後標識し，あらかじめ配列がデザインされたDNAオリゴマーを配置したチップと反応させ，専用のスキャナで信号を読み，配列を決定する方法である．筆者らは2006年時点でCMT原因遺伝子として確認されていた27遺伝子と新規遺伝子候補10遺伝子を搭載したCMT-DNAチップを作成した[19]．586本のPCR反応を32分割しmultiplex PCRにかけることで，時間と労力はかなり軽減でき，10万塩基の配列を決定するのに必要な時間は最短で2日間となっ

た．この手法を用いて，脱髄型CMTではFISH法で*PMP22*コピー数が正常だった症例を，また軸索型・中間型CMTでは全例を対象とし，2007年より網羅的遺伝子診断を行っている．

マイクロアレイDNAチップは，その仕組み上，挿入変異，欠失変異，リピート配列，重複変異に関しては検出し難い．比較的大きな欠失のホモ接合体であれば欠失部分のシグナルが消失するため，検出可能である．我々が用いているAffymetrix社製マイクロアレイDNAチップは一度デザイン/製作すると容易には仕様を変更できない問題点がある．新たに原因遺伝子を搭載したい場合，マイクロアレイDNAチップのデザインそのものから変更する必要がある．また，著者らの報告でも診断率が約20%程度と十分とはいえず，今後新しい試みの検討が必要であろう．現時点では，新規遺伝子を追加搭載し，DNAチップを更新していく方法がコスト的には有効と考えられるが，将来的には次世代ゲノムシークエンスの導入が必要であろう．次世代シークエンス法は，数千万から1000億塩基の配列を一度に決定する方法で，1ランでヒトゲノム全体を決定できる能力をもつ機種も登場している．ランニングコストが高い点や，データ量が膨大すぎる点などの問題点があり，個々の症例に対して解析を行うにはもう少し時間を要する．最近になり，1ランあたりのコストが比較的安価な機種が登場しており，将来はゲノムシークエンス法が遺伝子診断の主力になる可能性が高い．根本的な遺伝子異常を明らかにし，病態の解明および治療法へつなげていくためにも，網羅的遺伝子診断をさらに発展させていく必要がある．

文献

1) Lupski JR, Reid JG, Gonzaga-Jauregui C, et al. Whole-genome sequencing in a patient with Charcot-Marie-Tooth neuropathy. N Engl J Med. 2010; 362: 1181-91.
2) Roa BB, Garcia CA, Lupski JR. Charcot-Marie-Tooth disease type 1A: molecular mechanisms of gene dosage and point mutation underlying a common inherited peripheral neuropathy. Int J Neurol. 1991-1992; 25-26: 97-107.
3) Saporta ASD, Sottile SL, Shy ME, et al. Charcot-Marie-Tooth disease subtypes and genetic testing strategies. Ann Neurol. 2011; 69: 22-33.
4) Szigeti K, Nelis E, Lupski JR, et al. Molecular diagnostics of Charcot-Marie-Tooth disease and related peripheral neuropathies. Neuromolecular Med. 2006; 8: 243-54.
5) Ohnishi A, Li LY, Fukushima Y, et al. Asian hereditary neuropathy patients with peripheral myelin protein-22 gene aneuploidy. Am J Med Genet. 1995; 59: 51-8.
6) Boerkoel CF, Takashima H, Lupski JR, et al. Charcot-Marie-Tooth disease and related neuropathies: mutation distribution and genotype-phenotype correlation. Ann Neurol. 2002; 51: 190-201.
7) Abe A, Numakura C, Hayasaka K, et al. Molecular diagnosis and clinical onset of Charcot-Marie-Tooth disease in Japan. J Hum Genet. 2011; 56; 364-8.
8) 橋口昭大，徳永章子，髙嶋　博，他．シャルコー・マリー・トゥース病　200例のマイクロアレイDNAチップによる遺伝子診断．Peripheral Nerve. 2011; 22: 64-71.
9) Chow CY, Zhang Y, Dowling JJ, et al. Mutation of FIG4 causes neurodegeneration in the pale tremor mouse and patients with CMT4J. Nature. 2007; 448: 68-72.
10) Delague V, Jacquier A, Hamadouche T, et al. Mutations in FGD4 encoding the Rho GDP/GTP exchange factor FRABIN cause autosomal recessive Charcot-Marie-Tooth type 4H. Am J Hum Genet. 2007; 81: 1-16.
11) Hantke J, Chandler D, King R, et al. A mutation in an alternative untranslated exon of hexokinase 1 associated with hereditary motor and sensory neuropathy -- Russe (HMSNR). Eur J Hum Genet. 2009; 17: 1606-14.
12) Kim HJ, Sohn KM, Shy ME, et al. Mutations in PRPS1, which encodes the phosphoribosyl pyrophosphate synthetase enzyme critical for

nucleotide biosynthesis, cause hereditary peripheral neuropathy with hearing loss and optic neuropathy (cmtx5). Am J Hum Genet. 2007; 81: 552-8.

13) Leal A, Huehne K, Bauer F, et al. Identification of the variant Ala335Val of MED25 as responsible for CMT2B2: molecular data, functional studies of the SH3 recognition motif and correlation between wild-type MED25 and PMP22 RNA levels in CMT1A animal models. Neurogenetics. 2009; 10: 275-87.

14) Landoure G, Zdebik AA, Martinez TL, et al. Mutations in TRPV4 cause Charcot-Marie-Tooth disease type 2C. Nat Genet. 2010; 42: 170-4.

15) Latour P, Thauvin-Robinet C, Baudelet-Mery C, et al. A major determinant for binding and aminoacylation of tRNA(Ala) in cytoplasmic Alanyl-tRNA synthetase is mutated in dominant axonal Charcot-Marie-Tooth disease. Am J Hum Genet. 2010; 86: 77-82.

16) McLaughlin HM, Sakaguchi R, Liu C, et al. Compound heterozygosity for loss-of-function lysyl-tRNA synthetase mutations in a patient with peripheral neuropathy. Am J Hum Genet. 2010; 87: 560-6.

17) Sivakumar K, Kyriakides T, Puls I, et al. Phenotypic spectrum of disorders associated with glycyl-tRNA synthetase mutations. Brain. 2005; 128(Pt10): 2304-14.

18) Jordanova A, Irobi J, Thomas FP, et al. Disrupted function and axonal distribution of mutant tyrosyl-tRNA synthetase in dominant intermediate Charcot-Marie-Tooth neuropathy. Nat Genet. 2006; 38: 197-202.

19) 橋口昭大, 高嶋　博. シャルコー・マリー・トゥース病の診断: 遺伝子診断. Peripheral Nerve. 2011; 22: 2-11.

Annual Review 神経 2012 ©

発行 2012年 1月25日 初版 1刷

編集者 鈴木則宏
祖父江元
荒木信夫
宇川義一
川原信隆

発行者 株式会社 中外医学社
代表取締役 青木 滋

〒162-0805 東京都新宿区矢来町62
電話 03-3268-2701（代）
振替口座 00190-1-98814番

印刷/東京リスマチック（株） ＜TO・HU＞
製本/田中製本（株） Printed in Japan
ISBN978-4-498-12896-5

REPORT

The TRK-Fused Gene Is Mutated in Hereditary Motor and Sensory Neuropathy with Proximal Dominant Involvement

Hiroyuki Ishiura,[1] Wataru Sako,[3] Mari Yoshida,[4] Toshitaka Kawarai,[3] Osamu Tanabe,[3,5] Jun Goto,[1] Yuji Takahashi,[1] Hidetoshi Date,[1] Jun Mitsui,[1] Budrul Ahsan,[1] Yaeko Ichikawa,[1] Atsushi Iwata,[1] Hiide Yoshino,[6] Yuishin Izumi,[3] Koji Fujita,[3] Kouji Maeda,[3] Satoshi Goto,[3] Hidetaka Koizumi,[3] Ryoma Morigaki,[3] Masako Ikemura,[7] Naoko Yamauchi,[7] Shigeo Murayama,[8] Garth A. Nicholson,[9] Hidefumi Ito,[10] Gen Sobue,[11] Masanori Nakagawa,[12] Ryuji Kaji,[3,*] and Shoji Tsuji[1,2,13,*]

Hereditary motor and sensory neuropathy with proximal dominant involvement (HMSN-P) is an autosomal-dominant neurodegenerative disorder characterized by widespread fasciculations, proximal-predominant muscle weakness, and atrophy followed by distal sensory involvement. To date, large families affected by HMSN-P have been reported from two different regions in Japan. Linkage and haplotype analyses of two previously reported families and two new families with the use of high-density SNP arrays further defined the minimum candidate region of 3.3 Mb in chromosomal region 3q12. Exome sequencing showed an identical c.854C>T (p.Pro285-Leu) mutation in the TRK-fused gene (*TFG*) in the four families. Detailed haplotype analysis suggested two independent origins of the mutation. Pathological studies of an autopsied patient revealed TFG- and ubiquitin-immunopositive cytoplasmic inclusions in the spinal and cortical motor neurons. Fragmentation of the Golgi apparatus, a frequent finding in amyotrophic lateral sclerosis, was also observed in the motor neurons with inclusion bodies. Moreover, TAR DNA-binding protein 43 kDa (TDP-43)-positive cytoplasmic inclusions were also demonstrated. In cultured cells expressing mutant TFG, cytoplasmic aggregation of TDP-43 was demonstrated. These findings indicate that formation of TFG-containing cytoplasmic inclusions and concomitant mislocalization of TDP-43 underlie motor neuron degeneration in HMSN-P. Pathological overlap of proteinopathies involving TFG and TDP-43 highlights a new pathway leading to motor neuron degeneration.

Hereditary motor and sensory neuropathy with proximal dominant involvement (HMSN-P [MIM 604484]) is an autosomal-dominant disease characterized by predominantly proximal muscle weakness and atrophy followed by distal sensory disturbances.[1] HMSN-P was first described in patients from the Okinawa Islands of Japan, where more than 100 people are estimated to be affected.[2] Two Brazilian HMSN-P-affected families of Okinawan ancestry have also been reported.[3,4]

The disease onset is usually in the 40s and is followed by a slowly progressive course. Painful muscle cramps and abundant fasciculations are observed, particularly in the early stage of the disease. In contrast to the clinical presentations of other hereditary motor and sensory neuropathies (HMSNs) presenting with predominantly distal motor weakness reflecting axonal-length dependence, the clinical presentation of HMSN-P is unique in that it involves proximal predominant weakness with widespread fasciculations resembling those of amyotrophic lateral sclerosis (ALS).[5] Distal sensory loss is accompanied later in the disease course, but the degree of the sensory involvement varies among patients. Neuropathological findings revealed severe neuronal loss and gliosis in the spinal anterior horns and mild neuronal loss and gliosis in the hypoglossal and facial nuclei of the brainstem, which indicates that the primary pathological feature of HMSN-P is a motor neuronopathy involving motor neurons, but not a motor neuropathy involving axons.[1,5] The posterior column, corticospinal tract, and spinocerebellar tract showed loss of myelinated fibers and gliosis. Neuronal loss and gliosis were found in Clarke's nucleus. Dorsal root ganglia showed mild to marked neuronal loss.[1,5] These observations suggest that HMSN-P shares neuropathological findings in part with those observed in familial ALS.[6]

Previous studies on Okinawan kindreds mapped the disease locus to chromosome 3q.[1] Subsequently, we identified two large families (families 1 and 2 in Figure 1A) affected by quite a similar phenotype in the Kansai area of Japan, located in the middle of the main island of Japan and far distant from the Okinawa Islands. We mapped the

[1]Department of Neurology, The University of Tokyo Graduate School of Medicine, 7-3-1 Hongo, Bunkyo-ku, Tokyo 113-8655, Japan; [2]Medical Genome Center, The University of Tokyo Hospital, 7-3-1 Hongo, Bunkyo-ku, Tokyo 113-8655, Japan; [3]Department of Clinical Neuroscience, The Tokushima University Graduate School of Medicine, 3-18-15 Kuramoto-cho, Tokushima 770-8503, Japan; [4]Department of Neuropathology, Institute for Medical Science of Aging, Aichi Medical University, 21 Karimata, Iwasaku, Nagakute-shi, Aichi 480-1195, Japan; [5]Department of Cell and Developmental Biology, University of Michigan Medical School, 109 Zina Pitcher Place, Ann Arbor, MI 48109-2200, USA; [6]Yoshino Neurology Clinic, 3-3-16 Konodai, Ichikawa, Chiba 272-0827, Japan; [7]Department of Pathology, Graduate School of Medicine, The University of Tokyo, 7-3-1 Hongo, Bunkyo-ku, Tokyo 113-8655, Japan; [8]Department of Neuropathology and the Brain Bank for Aging Research, Tokyo Metropolitan Institute of Gerontology, 35-2 Sakae-cho, Itabashi-ku, Tokyo 173-0015, Japan; [9]Molecular Medicine Laboratory and ANZAC Research Institute, University of Sydney, Sydney NSW 2139, Australia; [10]Department of Neurology, Kyoto University Graduate School of Medicine, 54 Kawahara-cho, Shogoin, Sakyo-ku, Kyoto 606-8507, Japan; [11]Department of Neurology, Nagoya University Graduate School of Medicine, 65 Tsurumai-cho, Showa-ku, Nagoya-shi, Aichi 466-0065, Japan; [12]Department of Neurology and Gerontology, Kyoto Prefectural University Graduate School of Medicine, 465, Kajii-cho, Kamigyo-ku, Kyoto 602-0841, Japan; [13]Division of Applied Genetics, National Institute of Genetics, Yata 1111, Mishima, Shizuoka 11-8540, Japan
*Correspondence: tsuji@m.u-tokyo.ac.jp (S.T.), rkaji@clin.med.tokushima-u.ac.jp (R.K.)
http://dx.doi.org/10.1016/j.ajhg.2012.07.014.

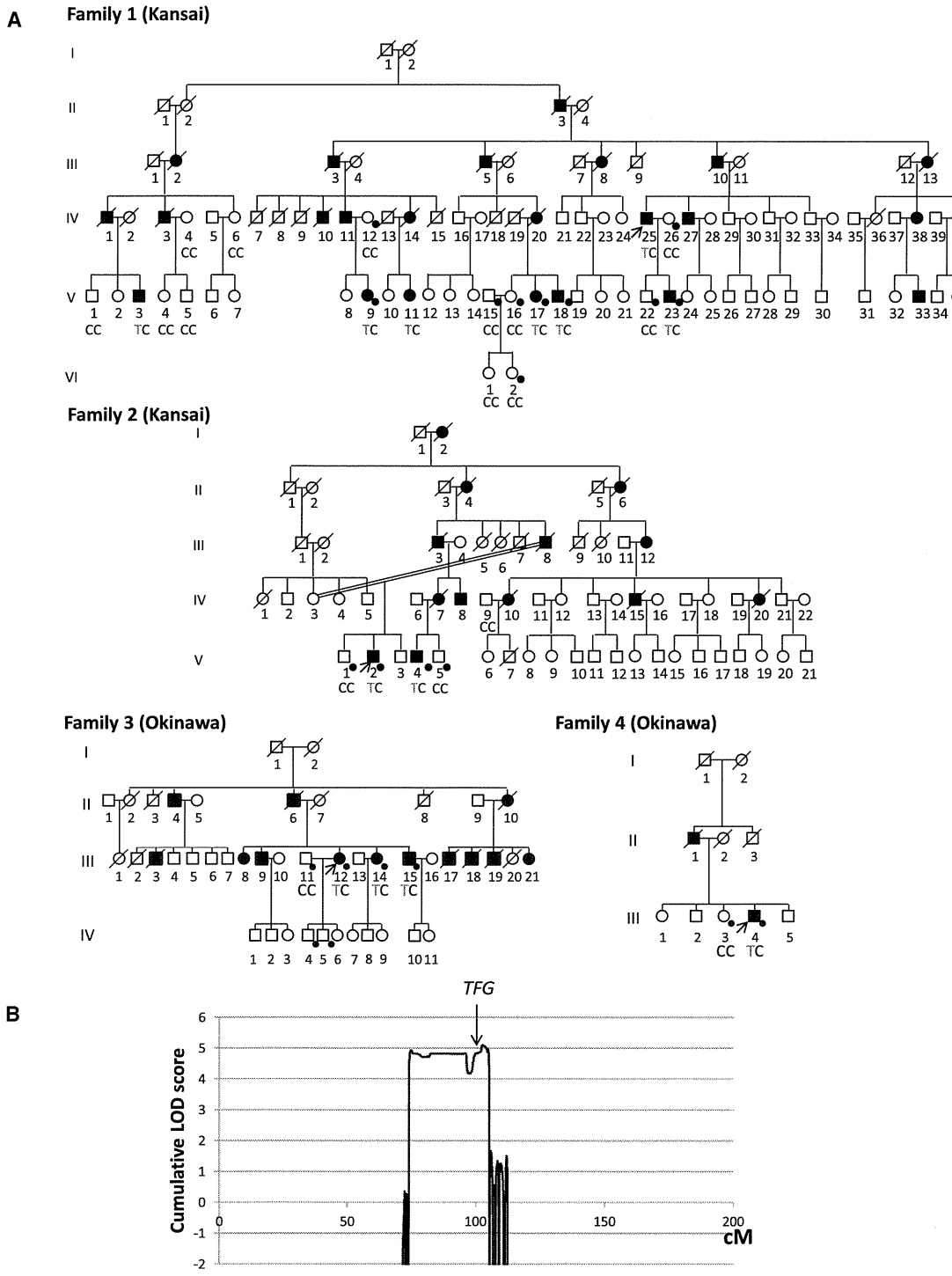

Figure 1. Pedigree Charts and Linkage Analysis
(A) Pedigree charts of families 1 and 2 (Kansai kindreds) and families 3 and 4 (Okinawan kindreds) are shown. Squares and circles indicate males and females, respectively. Affected persons are designated with filled symbols. A diagonal line through a symbol represents a deceased person. A person with an arrow is an index patient. Genotypes of *TFG* c.854 are shown in individuals in whom genomic DNA was analyzed. Individuals genotyped with SNP arrays for linkage analysis and haplotype reconstruction are indicated by dots. (B) Cumulative parametric multipoint LOD scores on chromosome 3 of all the families are shown.

disease locus to chromosome 3q,[7] overlapping with the previously defined locus, which strongly indicates that these diseases are indeed identical.

In addition to the large Kansai HMSN-P-affected families, we found two new Okinawan HMSN-P-affected families (families 3 and 4 in Figure 1A) in our study. In total, 9 affected and 15 unaffected individuals from the Kansai area and four affected and four unaffected individuals from the Okinawa Islands were enrolled in the study. Written informed consent was obtained from

Table 1. Clinical Characteristics of Patients with HMSN-P from Families 1 and 2 from Kansai and Families 3 and 4 from Okinawa

		Family 3			Family 4
	Families 1 and 2	**III-12**	**III-14**	**III-15**	**III-4**
Age at examination (years)	40s–50s	54	52	50	54
Age at onset (years)	37.5 ± 8	44	40	early 20s	41
Initial symptoms	shoulder dislocation and difficulty walking	proximal leg weakness	painful cramps	painful cramps and fasciculation	painful cramps and calf atrophy
Motor					
Proximal muscle weakness and atrophy	+	+	mild	+	+
Painful cramps	+	+	+	+	+
Fasciculations	+	+	+	+	+
Motor ability	bedridden after 10–20 years from disease onset	unable to walk; wheelchair	only mild difficulty climbing stairs	walk with effort	unable to walk; wheelchair
Bulbar symptoms	− ~ +	−	−	−	−
Sensory					
Dysesthesia	+	+	mild	+	+
Decreased tactile sensation	+	+	−	mild	+
Decreased vibratory sensation	+	mild	mild	mild	+
Reflexes					
Tendon reflexes	diminished	diminished	diminished	diminished	diminished
Pathological reflexes	−	−	−	−	−
Laboratory Tests and Electrophysiological Findings					
Serum creatine kinase level	270 ± 101 IU/l	761 IU/l	not measured	625 IU/l	399 IU/l
Hyperglycemia	4/13 patients	−	−	−	+
Hyperlipidemia	3/13 patients	+	−	+	+
Nerve conduction study	motor and sensory axonal degeneration	motor and sensory axonal degeneration	not examined	not examined	motor and sensory axonal degeneration
Needle electromyography	neurogenic changes with fibrillation potentials and positive sharp waves	neurogenic changes with fibrillation potentials and positive sharp waves	not examined	not examined	not examined

The clinical characteristics of the patients from families 1 and 2 were summarized in accordance with the previous studies.[5,6]

all participants. This study was approved by the institutional review boards at the University of Tokyo and the Tokushima University Hospital. Genomic DNA was extracted from peripheral-blood leukocytes or an autopsied brain according to standard procedures.

The clinical presentations of the patients from the four families are summarized in Table 1 and Table S1, available online. Characteristic painful cramps and fasciculations were noted at the initial stage of the disease in all the patients from the four families. Whereas some of the patients showed painful cramps in their 20s, the ages of onset of motor weakness (41.6 ± 2.9 years old) were quite uniform. These patients presented slowly progressive, predominantly proximal weakness and atrophy with diminished tendon reflexes in the lower extremities. Sensory impairment was generally mild. Indeed, one patient (III-4 in family 4) has been diagnosed with very slowly progressive ALS. Although frontotemporal dementia (FTD) is an occasionally observed clinical presentation in patients with ALS, dementia was not observed in these patients. Laboratory tests showed mildly elevated serum creatine kinase levels. Electrophysiological studies showed similar results in all the patients investigated and revealed a decreased number of motor units with abundant positive sharp waves, fibrillation, and fasciculation potentials. Sensory-nerve action potentials of the sural nerve were lost in the later stage of the disease. All these clinical findings were similar to those described in previous reports.[1,3,4]

To further narrow the candidate region, we conducted detailed genotyping by employing the Genome-Wide Human SNP array 6.0 (Affymetrix). Multipoint parametric linkage analysis and haplotype reconstruction were performed with the pipeline software SNP-HiTLink[8] and Allegro v.2[9] (Figure 1A). In addition to the SNP genotyping, we also used newly discovered polymorphic dinucleotide repeats for haplotype comparison (microsatellite marker 1 [MS1], chr3: 101,901,207–101,901,249; and MS2, chr3: 102,157,749–102,157,795 in hg18) around *TFG* (see Table S2 for primer sequences). The genome-wide linkage study revealed only one chromosome 3 region showing a cumulative LOD score exceeding 3.0 (Figure 1B), confirming the result of our previous study.[7] An obligate recombination event was observed between rs4894942 and rs1104964, thus further refining the telomeric boundary of the candidate region in Kansai families (Figure 2A). The Okinawan families (families 3 and 4) shared an extended disease haplotype spanning 3.3 Mb, consistent with a founder effect reported in the Okinawan HMSN-P-affected families,[1] thus defining the 3.3 Mb region as the minimum candidate region.

We then performed exon capture (Sequence Capture Human Exome 2.1 M Array [NimbleGen]) of the index patient from family 3 and subsequent passively parallel sequencing by using two lanes of GAIIx (100 bp single end [Illumina]) and a one-fifth slide of SOLiD 4 (50 bp single end [Life Technologies]). GAIIx and SOLiD4 yielded 2.60 and 2.76 Gb of uniquely mapped reads,[10] respectively. The average coverages were 29.0× and 26.8× in GAIIx and SOLiD4, respectively (Table S3 and Figure S1). In summary, 175,236 single nucleotide variants (SNVs) and 25,987 small insertions/deletions were called.[11] The numbers of exonic and splice-site variants were 14,189 and 127, respectively. In the minimum candidate region of 3.3 Mb, only 11 exonic SNVs were found, and only one was novel (i.e., not found in dbSNP) and nonsynonymous. Direct nucleotide-sequence analysis confirmed the presence of heterozygous SNV c.854C>T (p.Pro285Leu) in TRK-fused gene (*TFG* [NM_006070.5]) in all the patients from families 3 and 4 (Figure 3A and Figure S2[12]). Intriguingly, direct nucleotide-sequence analysis of all *TFG* exons (see Table S4 for primer sequences) of one patient from each of families 1 and 2 from the Kansai area revealed an identical c.854C>T (p.Pro285Leu) *TFG* mutation cosegregating with the disease (Figure 1A and Figure 3A). The base substitution was not observed in 482 Japanese controls (964 chromosomes), dbSNP, the 1000 Genomes Project Database, or the Exome Sequencing Project Database. Pro285 is located in the P/Q-rich domain in the C-terminal region of TFG (Figure 3B) and is evolutionally conserved (Figure 3C). PolyPhen predicts it to be "probably damaging." Because some of the exonic sequences were not sufficiently covered by exome sequencing (i.e., their read depths were no more than 10×) (Figure S1), direct nucleotide-sequence analysis was further conducted for these exonic sequences (Table S5). However, it did not reveal any other novel nonsynonymous variants, confirming that c.854C>T (p.Pro285Leu) is the only mutation exclusively present in the candidate region of 3.3 Mb. All together, we concluded that it was the disease-causing mutation.

Because we found an identical mutation in both Kansai (families 1 and 2) and Okinawan (families 3 and 4) families, we then compared the haplotypes with the c.854C>T (p.Pro285Leu) mutation in the Kansai and Okinawan families in detail. To obtain high-resolution haplotypes, we included custom-made markers, including MS1 and MS2, and new SNVs identified by our exome analysis, in addition to the high-density SNPs used in the linkage analysis. The two Kansai families shared as long as 24.0 Mb of haplotype, and the two Okinawan families shared 3.3 Mb, strongly supporting a common ancestry in each region. When the haplotypes of the Kansai and Okinawan families were compared, it turned out that these families do not share the same haplotype because the markers nearest to *TFG* are discordant at markers 48.5 kb centromeric and 677 bp telomeric to the mutation within a haploblock (Figure 2B). Although the possibility of rare recombination events just distal to the mutation cannot be completely excluded, as suggested by the population-based recombination map (Figure 2B), these findings strongly support the interpretation that the mutations have independent origins and provide further evidence that *TFG* contains the causative mutation for this disease.

Mutational analyses of *TFG* were further conducted in patients with other diseases affecting lower motor neurons (including familial ALS [n = 18], axonal HMSN [n = 26], and hereditary motor neuropathy [n = 3]) and revealed no mutations in *TFG*, indicating that c.854C>T (p.Pro285-Leu) in *TFG* is highly specific to HMSN-P.

In this study, we identified in all four families a single variant that appears to have developed on two different haplotypes. The mutation disrupts the PXXP motif, also known as the Src homology 3 (SH3) domain, which might affect protein-protein interactions. In addition, substitution of leucine for proline is expected to markedly alter the protein's secondary structure, which might substantially compromise the physiological functions of TFG.

By employing the primers shown in Table S6, we obtained full-length cDNAs by PCR amplification of the cDNAs prepared from a cDNA library of the human fetal brain (Clontech). During this process, four species of cDNA were identified (Figure S3A). To determine the relative abundance of these cDNA species, we used the primers shown in Table S7 to conduct fragment analysis of the RT-PCR products obtained from RNAs extracted from various tissues; these primers were designed to discriminate four cDNA species on the basis of the size of the PCR products. The analysis revealed that TFG is ubiquitously expressed, including in the spinal cord and dorsal root ganglia, which are the affected sites of HMSN-P (Figure S3B).

Neuropathological studies were performed in a *TFG*-mutation-positive patient (IV-25 in family 1) who died of

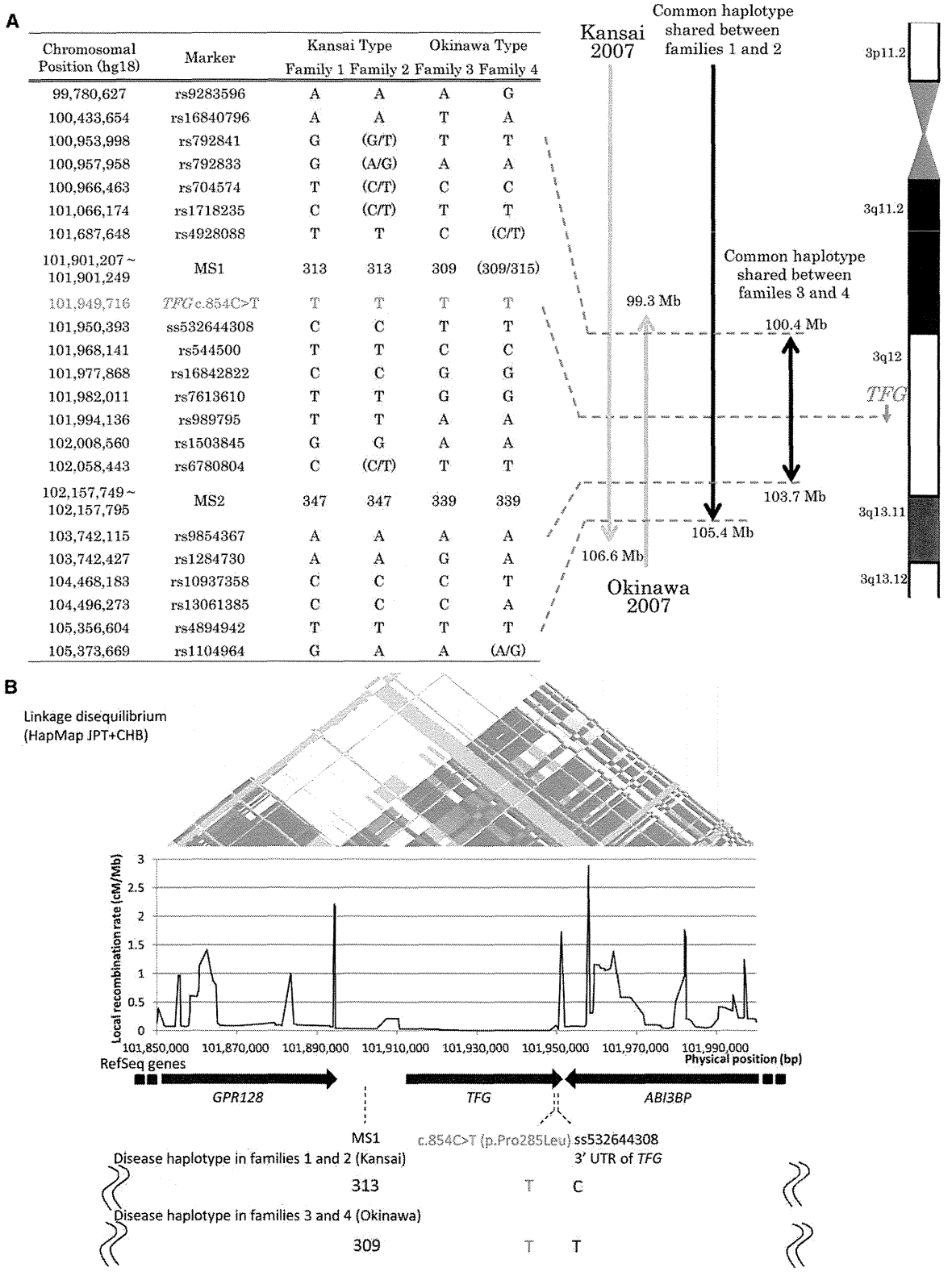

Figure 2. Haplotype Analysis and Minimum Candidate Region of HMSN-P

(A) Haplotypes were reconstructed for all the families with the use of SNP array data and microsatellite markers. Previously reported candidate regions are shown as "Kansai 2007" and "Okinawa 2007."[1,6] Because families 1 and 2 are distantly related, an extended shared common haplotype was observed on chromosome 3, as indicated by a previous study.[6] A reassessment of linkage analysis with high-density SNP markers revealed a recombination between rs4894942 and rs1104964 in family 2, thus refining the telomeric boundary of the candidate region in Kansai families (designated as "Common haplotype shared between families 1 and 2). Furthermore, a shared common haplotype (3.3 Mb with boundaries at rs16840796 and rs1284730) between families 3 and 4 was found, defining the minimum candidate region.

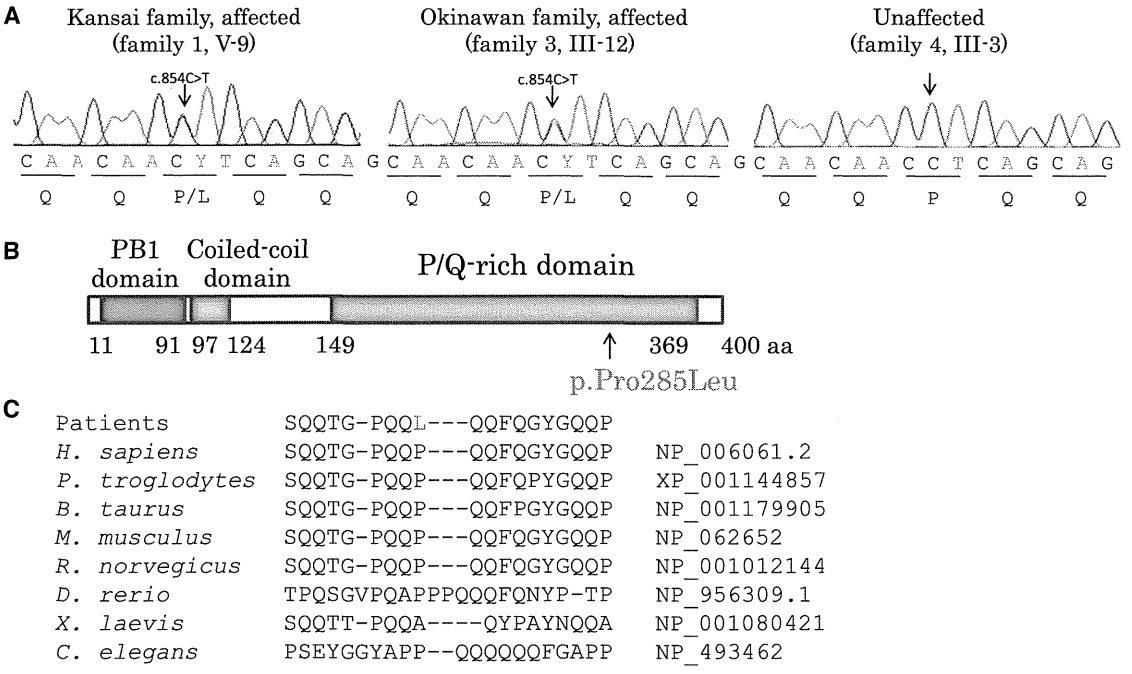

Figure 3. Identification of Causative Mutation
(A) Exome sequencing revealed that only one novel nonsynonymous variant is located within the minimum candidate region. Direct nucleotide-sequence analysis confirmed the mutation, c.854C>T (p.Pro285Leu), in *TFG* in both Kansai and Okinawan families. The mutation cosegregated with the disease (Figure 1A).
(B) Schematic representation of TFG isoform 1. The alteration (p.Pro285Leu) detected in this study is shown below.
(C) Cross-species homology search of the partial TFG amino acid sequence containing the p.Pro285Leu alteration revealed that Pro285 is evolutionally conserved among species.

pneumonia at 67 years of age.[5] Immunohistochemical observations employing a TFG antibody (Table S8) revealed fine granular immunostaining of TFG in the cytoplasm of motor neurons in the spinal cord of neurologically normal controls (n = 3; age at death = 58.7 ± 19.6 years old) (Figure 4A). In the HMSN-P patient, in contrast, TFG-immunopositive inclusion bodies were detected in the motor neurons of the facial, hypoglossal, and abducens nuclei and the spinal cord, as well as in the sensory neurons of the dorsal root ganglia, but were not detected in glial cells (Figures 4B–4D). A small number of cortical neurons in the precentral gyrus also showed TFG-immunopositive inclusion bodies (Figure 4E). Serial sections stained with antibodies against ubiquitin or TFG (Figure 4F) and double immunofluorescence staining (Figure 4G) demonstrated that TFG-immunopositive inclusions colocalized with ubiquitin deposition. Inclusion bodies were immunopositive for optineurin in motor neurons of the brainstem nuclei and the anterior horn of the spinal cord,[5] as well as in sensory neurons of the dorsal root ganglia (data not shown). These data strongly indicate that HMSN-P is a proteinopathy involving TFG.

Because HMSN-P and ALS share some clinical characteristics, we then examined whether neuropathological findings of HMSN-P shared cardinal features with those of sporadic ALS.[13–16] Immunohistochemistry with a TDP-43 antibody revealed skein-like inclusions in the remaining motor neurons of the abducens nucleus and the anterior horn of the lumbar cord (Figures 4H–4I). Phosphorylated TDP-43-positive inclusions were also identified in neurons of the anterior horn of the cervical cord and Clarke's nucleus (Figures 4J–4K). In contrast, TFG immunostaining of spinal-cord specimens from four patients with sporadic ALS (their age at death was 72.3 ± 7.4 years old) revealed no pathological staining in the motor neurons (data not shown). Double immunofluorescence staining revealed that many of the TFG-immunopositive round inclusions in the HSMN-P patient were negative for TDP-43 (Figure 4L), whereas a small number of inclusions were positive for both TFG and TDP-43 (Figure 4M). In addition, to investigate morphological Golgi-apparatus changes, which have recently been found in motor neurons of autopsied tissues of ALS patients,[17] we conducted immunohistochemical analysis by using

(B) Disease haplotypes in the Kansai and Okinawan kindreds are indicated below. Local recombination rates, RefSeq genes, and the linkage disequilibrium map from HapMap JPT (Japanese in Tokyo, Japan) and CHB (Han Chinese in Beijing, China) samples are shown above the disease haplotypes. When disease haplotypes of the Kansai and Okinawan kindreds are compared, the markers nearest to *TFG* are discordant at markers 48.5 kb centromeric and 677 bp telomeric to the mutation within a haploblock, strongly supporting the interpretation that the mutations have independent origins.

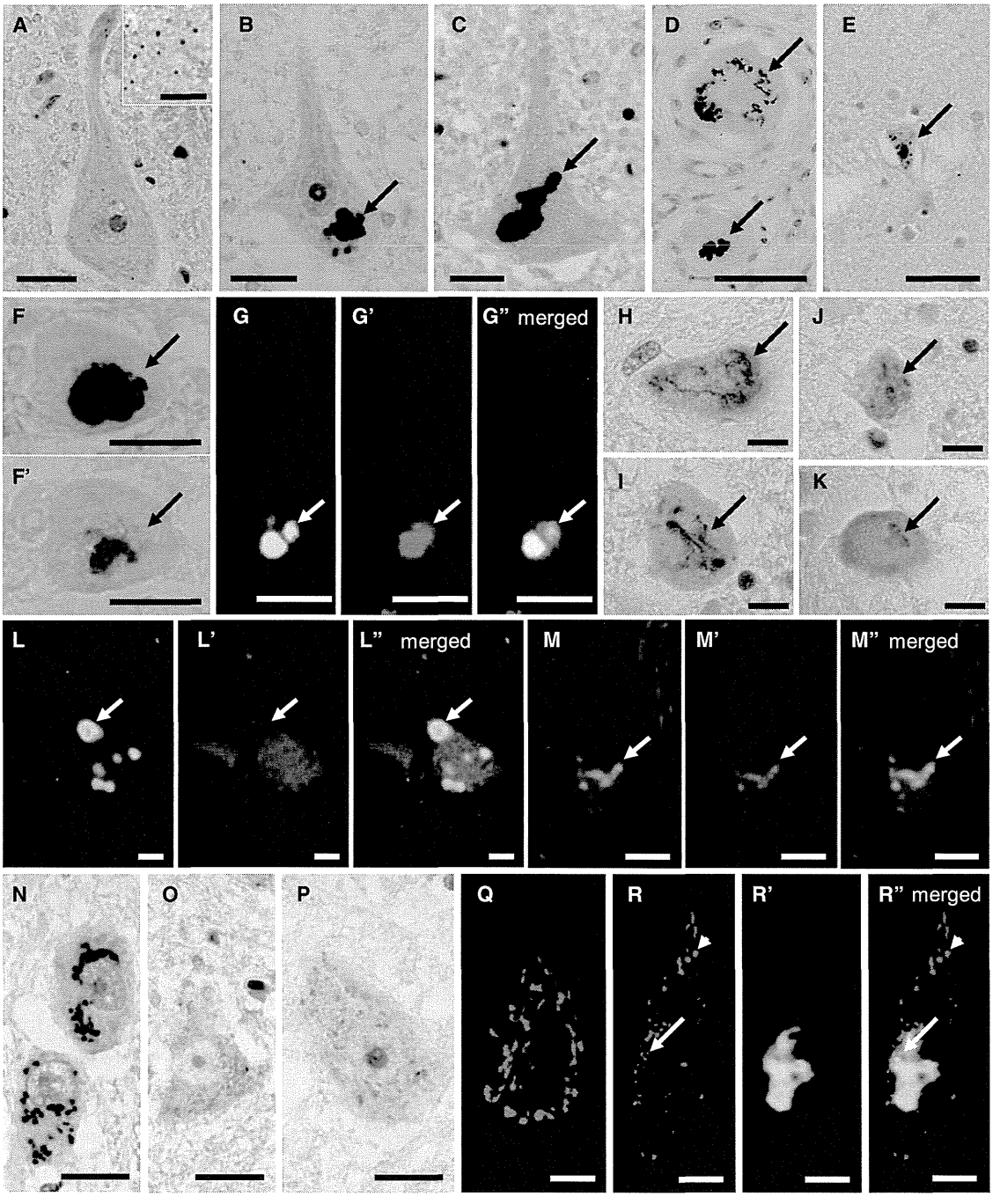

Figure 4. TFG-Related Neuropathological Findings

(A) TFG immunostaining (with hematoxylin counterstaining) of a motor neuron in the spinal cord of a neurologically normal control. A high-power magnified photomicrograph (inset) shows fine granular staining of TFG in the cytoplasm. The scale bars represent 20 μm (main panel) and 10 μm (inset).

(B–E) TFG-immunopositive inclusions of the neurons (with hematoxylin counterstaining) in the hypoglossal nucleus (B), anterior horn of the spinal cord (C), dorsal root ganglion (D, arrows), and motor cortex (E, arrow) of the patient with the *TFG* mutation. The scale bars represent 20 μm (B–D) and 50 μm (E).

(F and F′) Serial section analysis of the facial nucleus motor neuron showing an inclusion body colabeled for TFG (F) and ubiquitin (F′). The scale bars represent 20 μm.

(G–G″) Double immunofluorescence microscopy confirming colocalization of TFG (green) and ubiquitin (red) in an inclusion body of a motor neuron in the hypoglossal nucleus. The scale bars represent 20 μm.

(H and I) TDP-43-positive skein-like inclusions in the motor neurons of the abducens nucleus (H) and anterior horn of the lumbar cord (I). The scale bars represent 20 μm.

(J and K) Phosporylated TDP-43-positive inclusion bodies in the cervical anterior horn (J) and Clarke's nucleus (K). The scale bars represent 20 μm.

(L–L″) Round inclusions (arrows) positive for TFG (green) but negative for TDP-43 (red). The scale bars represent 20 μm.

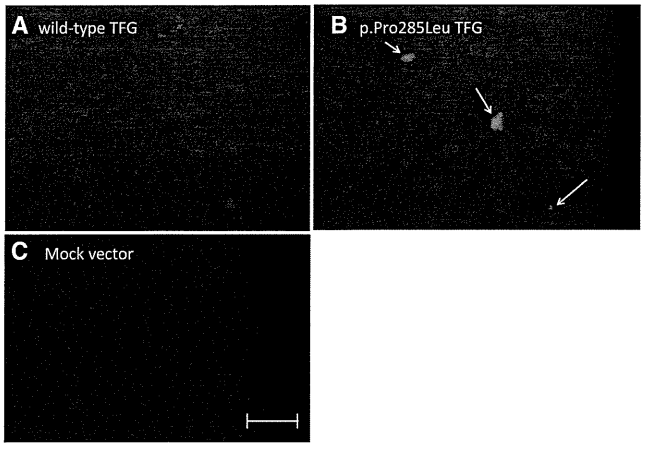

Figure 5. Formation of Cytoplasmic TDP-43 Aggregation Bodies in Cells Stably Expressing Mutant p.Pro285Leu TFG
The coding sequence of *TFG* cDNA was subcloned into pBluescript (Stratagene). After site-directed mutagenesis with a primer pair shown in Table S9, the mutant cDNAs were cloned into the BamHI and XhoI sites of pcDNA3 (Life Technologies). Stable cell lines were established by Lipofectamine (Life Technologies) transfection according to the manufacturer's instructions. Established cell lines were cultured under the ordinary cell-culture conditions (37°C and 5% CO_2) for 5–6 days and were subjected to immunocytochemical analyses. Neuro-2a cells stably expressing wild-type TFG (A), mutant TFG (p.Pro285Leu) (B), and a mock vector (C) are shown. TDP-43-immunopositive cytoplasmic inclusions are absent in the cells stably expressing wild-type TFG or the mock vector (A and C); however, TDP-43-immunopositive cytoplasmic inclusions were exclusively demonstrated in cells stably expressing mutant TFG (p.Pro285Leu), as indicated by arrows (B). Similar results were obtained with HEK 293 cells (not shown). Scale bars represent 10 μm.

a TGN46 antibody. It revealed that the Golgi apparatus was fragmented in approximately 70% of the remaining motor neurons in the lumbar anterior horn. The fragmentation of the Golgi apparatus was prominent near TFG-positive inclusion bodies (Figures 4N–4R). In summary, we found abnormal TDP-43-immunopositive inclusions in the cytoplasm of motor neurons, as well as fragmentation of the Golgi apparatus in HMSN-P, confirming the overlapping neuropathological features between HMSN-P and sporadic ALS.

To further investigate the effect of mutant TFG in cultured cells, stable cell lines expressing wild-type and mutant TFG (p.Pro285Leu) were established from neuro-2a and human embryonic kidney (HEK) 293 cells as previously described.[18] Established cell lines were cultured under the ordinary cell-culture conditions (37°C and 5% CO_2) for 5–6 days and were subjected to immunocytochemical analyses. The neuro-2a cells stably expressing wild-type or mutant TFG demonstrated no distinct difference in the distribution of endogenous TFG, FUS, or OPTN (data not shown). In contrast, cytoplasmic inclusions containing endogenous TDP-43 were exclusively observed in the neuro-2a cells stably expressing untagged mutant TFG, but not in those expressing wild-type TFG (Figure 5). Similar data were obtained from HEK 293 cells (data not shown). Thus, the expression of mutant TFG leads to mislocalization and inclusion-body formation of TDP-43 in cultured cells.

TFG was originally identified as a part of fusion oncoproteins (NTRK1-T3 in papillary thyroid carcinoma,[19] TFG-ALK in anaplastic large cell lymphoma,[20] and TFG/NOR1 in extraskeletal myxoid chondrosarcoma[21]), where the N-terminal portions of TFG are fused to the C terminus of tyrosine kinases or a superfamily of steroid-thyroid hormone-retinoid receptors acting as a transcriptional activator leading to the formation of oncogenic products. Very recently, TFG-1, a homolog of TFG in *Caenorhabditis elegans*, and TFG have been discovered to localize in endoplasmic-reticulum exit sites. TFG-1 acts in a hexameric form that binds the scaffolding protein Sec16 complex assembly and plays an important role in protein secretion with COPII-coated vesicles.[22] It is noteworthy that mutations in genes involved in vesicle trafficking[23,24] (such genes include *VAPB*, *CHMP2B*, *alsin*, *FIG4*, *VPS33B*, *PIP5K1C*, and *ERBB3*) cause motor neuron diseases, emphasizing the role of vesicle trafficking in motor neuron diseases. Thus, altered vesicle trafficking due to the *TFG* mutation might be involved in the motor neuron degeneration in HMSN-P. The presence of TFG-immunopositive inclusions in motor neurons raises the possibility that mutant TFG results in the misfolding and formation of cytoplasmic aggregate bodies, as well as altered vesicle trafficking.

An intriguing neuropathological finding is TDP-43-positive cytoplasmic inclusions in the motor neurons; these inclusions have recently been established as the fundamental neuropathological findings in ALS.[13,14] Of note, expression of mutant, but not wild-type, TFG in cultured cells led to the formation of TDP-43-containing cytoplasmic aggregation. These observations are similar

(M–M″) An inclusion immunopositive for both TFG (green) and TDP-43 (red) is observed in a small number of neurons. The scale bars represent 20 μm.
(N) Normal Golgi apparatus in the neurons of the intact thoracic intermediolateral nucleus. The scale bar represents 20 μm.
(O and P) Fragmentation of the Golgi apparatus with small, round, and disconnected profiles in the affected motor neurons of the lumbar anterior horn. The scale bars represent 20 μm.
(Q–R″) Immunohistochemical observations of the Golgi apparatus and TFG-immunopositive inclusions employing antibodies against TGN46 (red) and TFG (green), respectively. The scale bars represent 10 μm.
(Q) Normal size and distribution (red) in a motor neuron without inclusions.
(R–R″) The Golgi apparatus was fragmented into various sizes and reduced in number in the lumbar anterior horn motor neuron with TFG-positive inclusions (green). The fragmentation predominates near the inclusion (arrow), whereas the Golgi apparatuses distant from the inclusion showed nearly normal patterns (arrow head).

to what has been described for ALS, where TDP-43 is mislocalized from the normally localized nucleus to the cytoplasm with concomitant cytoplasmic inclusions. Cytoplasmic TDP-43 accumulation and inclusion formation have also been observed in motor neurons in familial ALS with mutations in *VAPB* (MIM 608627) or *CHMP2B* (MIM 600795).[25,26] Furthermore, TDP-43 pathology has been demonstrated in transgenic mice expressing mutant VAPB.[27] Although the mechanisms of mislocalization of TDP-43 remain to be elucidated, these observations suggest connections between alteration of vesicle trafficking and mislocalization of TDP-43. Thus, common pathophysiologic mechanisms might underlie motor neuron degenerations involving vesicle trafficking including TFG, as well as VAPB and CHMP2B. Because TDP-43 is an RNA-binding protein, RNA dysregulation has been suggested to play important roles in the TDP43-mediated neurodegeneration.[28] Furthermore, recent discovery of hexanucleotide repeat expansions in *C9ORF72* in familial and sporadic ALS/FTD (MIM 105550)[29,30] emphasizes the RNA-mediated toxicities as the causal mechanisms of neurodegeneration. Observations of TDP-43-positive cytoplasmic inclusions in the motor neurons of the patient with HMSN-P raise the possibility that RNA-mediated mechanisms might also be involved in motor neuron degeneration in HMSN-P.

In summary, we have found that *TFG* mutations cause HMSN-P. The presence of TFG/ubiquitin- and/or TDP-43-immunopositive cytoplasmic inclusions in motor neurons and cytosolic aggregation composed of TDP-43 in cultured cells expressing mutant TFG indicate a novel pathway of motor neuron death.

Supplemental Data

Supplemental Data include three figures and nine tables and can be found with this article online at http://www.cell.com/AJHG/.

Acknowledgments

The authors thank the families for participating in the study. We also thank the doctors who obtained clinical information of the patients. This work was supported in part by Grants-in-Aid for Scientific Research on Innovative Areas (22129002); the Global Centers of Excellence Program; the Integrated Database Project; Scientific Research (A) (B21406026) and Challenging Exploratory Research (23659458) from the Ministry of Education, Culture, Sports, Science, and Technology of Japan; a Grant-in-Aid for Research on Intractable Diseases and Comprehensive Research on Disability Health and Welfare from the Ministry of Health, Labour, and Welfare, Japan; Grants-in-Aid from the Research Committee of CNS Degenerative Diseases; the Ministry of Health, Labour, and Welfare of Japan; the Charcot-Marie-Tooth Association; and the National Medical Research Council of Australia. H.I. was supported by a Research Fellowship from the Japan Society for the Promotion of Science for Young Scientists. We also thank S. Ogawa (Cancer Genomics Project, The University of Tokyo) for his kind help in the analyses employing GAIIx and SOLiD4.

Received: April 16, 2012
Revised: May 27, 2012
Accepted: July 2, 2012
Published online: August 9, 2012

Web Resources

The URLs for data presented herein are as follows.

1000 Genomes Project Database, http://www.1000genomes.org/
dbSNP, http://www.ncbi.nlm.nih.gov/projects/SNP/
HapMap, http://hapmap.ncbi.nlm.nih.gov/
NHLBI GO Exome Sequencing Project, https://esp.gs.washington.edu/drupal/
Online Mendelian Inheritance in Man (OMIM), http://www.omim.org
PolyPhen, http://genetics.bwh.harvard.edu/pph/
RefSeq, http://www.ncbi.nlm.nih.gov/projects/RefSeq/
UCSC Human Genome Browser, http://genome.ucsc.edu/

References

1. Takashima, H., Nakagawa, M., Nakahara, K., Suehara, M., Matsuzaki, T., Higuchi, I., Higa, H., Arimura, K., Iwamasa, T., Izumo, S., and Osame, M. (1997). A new type of hereditary motor and sensory neuropathy linked to chromosome 3. Ann. Neurol. *41*, 771–780.
2. Nakagawa, M. (2009). [Wide spectrum of hereditary motor sensory neuropathy (HMSN)]. Rinsho Shinkeigaku *49*, 950–952.
3. Maeda, K., Sugiura, M., Kato, H., Sanada, M., Kawai, H., and Yasuda, H. (2007). Hereditary motor and sensory neuropathy (proximal dominant form, HMSN-P) among Brazilians of Japanese ancestry. Clin. Neurol. Neurosurg. *109*, 830–832.
4. Patroclo, C.B., Lino, A.M., Marchiori, P.E., Brotto, M.W., and Hirata, M.T. (2009). Autosomal dominant HMSN with proximal involvement: new Brazilian cases. Arq. Neuropsiquiatr. *67* (3B), 892–896.
5. Fujita, K., Yoshida, M., Sako, W., Maeda, K., Hashizume, Y., Goto, S., Sobue, G., Izumi, Y., and Kaji, R. (2011). Brainstem and spinal cord motor neuron involvement with optineurin inclusions in proximal-dominant hereditary motor and sensory neuropathy. J. Neurol. Neurosurg. Psychiatry *82*, 1402–1403.
6. Takahashi, H., Makifuchi, T., Nakano, R., Sato, S., Inuzuka, T., Sakimura, K., Mishina, M., Honma, Y., Tsuji, S., and Ikuta, F. (1994). Familial amyotrophic lateral sclerosis with a mutation in the Cu/Zn superoxide dismutase gene. Acta Neuropathol. *88*, 185–188.
7. Maeda, K., Kaji, R., Yasuno, K., Jambaldorj, J., Nodera, H., Takashima, H., Nakagawa, M., Makino, S., and Tamiya, G. (2007). Refinement of a locus for autosomal dominant hereditary motor and sensory neuropathy with proximal dominancy (HMSN-P) and genetic heterogeneity. J. Hum. Genet. *52*, 907–914.
8. Fukuda, Y., Nakahara, Y., Date, H., Takahashi, Y., Goto, J., Miyashita, A., Kuwano, R., Adachi, H., Nakamura, E., and Tsuji, S. (2009). SNP HiTLink: A high-throughput linkage analysis system employing dense SNP data. BMC Bioinformatics *10*, 121.
9. Gudbjartsson, D.F., Thorvaldsson, T., Kong, A., Gunnarsson, G., and Ingolfsdottir, A. (2005). Allegro version 2. Nat. Genet. *37*, 1015–1016.

10. Li, H., and Durbin, R. (2009). Fast and accurate short read alignment with Burrows-Wheeler transform. Bioinformatics *25*, 1754–1760.
11. Li, H., Handsaker, B., Wysoker, A., Fennell, T., Ruan, J., Homer, N., Marth, G., Abecasis, G., and Durbin, R.; 1000 Genome Project Data Processing Subgroup. (2009). The Sequence Alignment/Map format and SAMtools. Bioinformatics *25*, 2078–2079.
12. Robinson, J.T., Thorvaldsdóttir, H., Winckler, W., Guttman, M., Lander, E.S., Getz, G., and Mesirov, J.P. (2011). Integrative genomics viewer. Nat. Biotechnol. *29*, 24–26.
13. Neumann, M., Sampathu, D.M., Kwong, L.K., Truax, A.C., Micsenyi, M.C., Chou, T.T., Bruce, J., Schuck, T., Grossman, M., Clark, C.M., et al. (2006). Ubiquitinated TDP-43 in frontotemporal lobar degeneration and amyotrophic lateral sclerosis. Science *314*, 130–133.
14. Arai, T., Hasegawa, M., Akiyama, H., Ikeda, K., Nonaka, T., Mori, H., Mann, D., Tsuchiya, K., Yoshida, M., Hashizume, Y., and Oda, T. (2006). TDP-43 is a component of ubiquitin-positive tau-negative inclusions in frontotemporal lobar degeneration and amyotrophic lateral sclerosis. Biochem. Biophys. Res. Commun. *351*, 602–611.
15. Hasegawa, M., Arai, T., Nonaka, T., Kametani, F., Yoshida, M., Hashizume, Y., Beach, T.G., Buratti, E., Baralle, F., Morita, M., et al. (2008). Phosphorylated TDP-43 in frontotemporal lobar degeneration and amyotrophic lateral sclerosis. Ann. Neurol. *64*, 60–70.
16. Inukai, Y., Nonaka, T., Arai, T., Yoshida, M., Hashizume, Y., Beach, T.G., Buratti, E., Baralle, F.E., Akiyama, H., Hisanaga, S., and Hasegawa, M. (2008). Abnormal phosphorylation of Ser409/410 of TDP-43 in FTLD-U and ALS. FEBS Lett. *582*, 2899–2904.
17. Stieber, A., Chen, Y., Wei, S., Mourelatos, Z., Gonatas, J., Okamoto, K., and Gonatas, N.K. (1998). The fragmented neuronal Golgi apparatus in amyotrophic lateral sclerosis includes the trans-Golgi-network: Functional implications. Acta Neuropathol. *95*, 245–253.
18. Kuroda, Y., Sako, W., Goto, S., Sawada, T., Uchida, D., Izumi, Y., Takahashi, T., Kagawa, N., Matsumoto, M., Matsumoto, M., et al. (2012). Parkin interacts with Klokin1 for mitochondrial import and maintenance of membrane potential. Hum. Mol. Genet. *21*, 991–1003.
19. Greco, A., Mariani, C., Miranda, C., Lupas, A., Pagliardini, S., Pomati, M., and Pierotti, M.A. (1995). The DNA rearrangement that generates the TRK-T3 oncogene involves a novel gene on chromosome 3 whose product has a potential coiled-coil domain. Mol. Cell. Biol. *15*, 6118–6127.
20. Hernández, L., Pinyol, M., Hernández, S., Beà, S., Pulford, K., Rosenwald, A., Lamant, L., Falini, B., Ott, G., Mason, D.Y., et al. (1999). TRK-fused gene (TFG) is a new partner of ALK in anaplastic large cell lymphoma producing two structurally different TFG-ALK translocations. Blood *94*, 3265–3268.
21. Hisaoka, M., Ishida, T., Imamura, T., and Hashimoto, H. (2004). TFG is a novel fusion partner of NOR1 in extraskeletal myxoid chondrosarcoma. Genes Chromosomes Cancer *40*, 325–328.
22. Witte, K., Schuh, A.L., Hegermann, J., Sarkeshik, A., Mayers, J.R., Schwarze, K., Yates, J.R., 3rd, Eimer, S., and Audhya, A. (2011). TFG-1 function in protein secretion and oncogenesis. Nat. Cell Biol. *13*, 550–558.
23. Dion, P.A., Daoud, H., and Rouleau, G.A. (2009). Genetics of motor neuron disorders: New insights into pathogenic mechanisms. Nat. Rev. Genet. *10*, 769–782.
24. Andersen, P.M., and Al-Chalabi, A. (2011). Clinical genetics of amyotrophic lateral sclerosis: What do we really know? Nat Rev Neurol *7*, 603–615.
25. Ince, P.G., Highley, J.R., Kirby, J., Wharton, S.B., Takahashi, H., Strong, M.J., and Shaw, P.J. (2011). Molecular pathology and genetic advances in amyotrophic lateral sclerosis: an emerging molecular pathway and the significance of glial pathology. Acta Neuropathol. *122*, 657–671.
26. Cox, L.E., Ferraiuolo, L., Goodall, E.F., Heath, P.R., Higginbottom, A., Mortiboys, H., Hollinger, H.C., Hartley, J.A., Brockington, A., Burness, C.E., et al. (2010). Mutations in CHMP2B in lower motor neuron predominant amyotrophic lateral sclerosis (ALS). PLoS ONE *5*, e9872.
27. Tudor, E.L., Galtrey, C.M., Perkinton, M.S., Lau, K.-F., De Vos, K.J., Mitchell, J.C., Ackerley, S., Hortobágyi, T., Vámos, E., Leigh, P.N., et al. (2010). Amyotrophic lateral sclerosis mutant vesicle-associated membrane protein-associated protein-B transgenic mice develop TAR-DNA-binding protein-43 pathology. Neuroscience *167*, 774–785.
28. Lee, E.B., Lee, V.M., and Trojanowski, J.Q. (2012). Gains or losses: Molecular mechanisms of TDP43-mediated neurodegeneration. Nat. Rev. Neurosci. *13*, 38–50.
29. DeJesus-Hernandez, M., Mackenzie, I.R., Boeve, B.F., Boxer, A.L., Baker, M., Rutherford, N.J., Nicholson, A.M., Finch, N.A., Flynn, H., Adamson, J., et al. (2011). Expanded GGGGCC hexanucleotide repeat in noncoding region of C9ORF72 causes chromosome 9p-linked FTD and ALS. Neuron *72*, 245–256.
30. Renton, A.E., Majounie, E., Waite, A., Simón-Sánchez, J., Rollinson, S., Gibbs, J.R., Schymick, J.C., Laaksovirta, H., van Swieten, J.C., Myllykangas, L., et al; ITALSGEN Consortium. (2011). A hexanucleotide repeat expansion in C9ORF72 is the cause of chromosome 9p21-linked ALS-FTD. Neuron *72*, 257–268.